Seismic Performance of Polypropylene Fiber Reinforced Cement Composite Bridge Columns

Kazuhiko Kawashima
Professor Emeritus, Tokyo Institute of Technology
Tokyo, Japan

ABSTRACT: This study investigates the effect of polypropylene fiber reinforced cement composites (PFRC) for enhancing the damage control and ductility capacity of a 7.5 m tall, 1.8 m by 1.8 m square bridge column subjected to 80% of the original intensity of the near-field ground motion recorded at the JR Takatori station during the 1995 Kobe, Japan earthquake using the E-Defense shake table. PFRC is a mixture of cement mortar and short discontinuous polypropylene fibers. Compared to the brittle failure of concrete in tension, PFRC exhibits ductile failure due to the formation of closely spaced micro cracks and the bridging action of fibers. The use of PFRC at the plastic hinge region mitigated cover and core concrete damage, local buckling of longitudinal bars and deformation of ties even after six times of repeated excitation. The damage sustained was much less than the normal damage of regular reinforced concrete columns.

1 INTRODUCTION

A large scale bridge experimental program was conducted in 2007-2010 by the National Research Institute for Earth Science and Disaster Prevention (NIED), Japan (Nakashima et al. 2008). In the program, shake table experiments were conducted for two typical reinforced concrete columns which failed during the 1995 Kobe, Japan earthquake (C1-1 and C1-2 experiments), a typical reinforced concrete column designed in accordance with the 2002 Japan design code (JRA 2002) (C1-5 experiment) and a new generation column using polypropylene fiber reinforced cement composites for enhancing the damage control and ductility (C1-6 experiment). The experiments were conducted using the E-Defense shake table where the table is 20 m by 15 m and has a payload of 1200 tf (12 MN). The maximum stroke of the table is 1 m and 0.5 m in the lateral and vertical directions, respectively. It was designed so that the ground motions during the 1995 Kobe earthquake can be generated.

C1-5 experiment was conducted using the E-Defense shake table with a ground motion 80% of the original intensity of the near-field ground motion recorded at the JR Takatori station during the 1995 Kobe earthquake. This is referred herein as the E-Takatori ground motion. The column performed satisfactorily under this ground motion. However, when the excitations were repeated under much stronger intensity and longer duration near-field ground motion, the column suffered extensive damage with blocks of crushed core concrete spilling out like explosion from the steel cage (Kawashima et al. 2010). Such failure was never seen in past quasi-static cyclic or hybrid loading experiments. Therefore, it is expected to develop columns which contribute to construct damage free bridges using materials that mitigate such damage under severe seismic loading.

Prior to the C1-6 experiment, a series of cyclic loading experiments were conducted on 1.68 m high, 0.4 m by 0.4 m square cantilever regular high strength concrete column and a column each using steel fiber reinforced concrete and polypropylene fiber reinforced cement composite at the plastic hinge region and the footing for deciding the material of C1-6 column (Kawashima

et al. 2011). The polypropylene fiber reinforced cement composite column had superior performance in mitigating cover and core concrete damage, longitudinal bar buckling and deformation of tie bars at the plastic hinge region resulting from the crack control capability of polypropylene fiber reinforced cement composite. As a result, C1-6 column was built using polypropylene fiber reinforced cement composite at the plastic hinge region and a part of the footing.

High performance fiber reinforced cement composites (HPFRCC) are materials that exhibit multiple fine cracks upon loading in tension which leads to improvement in toughness, fatigue resistance and deformation capacity (Matsumoto & Mihashi 2002). Engineered cementitious composites (ECC) is an HPRCC that has tensile strain capacity of about 0.03 to 0.05 resulting from the formation of closely spaced micro cracks due to the bridging action of fibers (Li & Leung, 1992). It has low elastic stiffness compared to concrete, and larger strain at peak compressive strength, due to the absence of course aggregates (Li et al. 1995). Polypropylene fiber reinforced cement composites, referred herein as PFRC, belongs to the class of ECC.

Previous investigations have shown the positive effects of using HPFRCC for structural members subjected to seismic loads. Kosa et al. (2007) examined the use of this material with polyvinyl alcohol (PVA) fibers for the seismic strengthening of scaled bridge piers similar to concrete jacketing. They found that a pier using PVA-HPFRCC on the cover concrete can provide confinement effect as much as the pier whose entire cross section was constructed of this material. Furthermore, the deformation capacity and the energy absorption capacity were also significantly improved compared with a pier constructed of ordinary concrete.

Saiidi et al. (2009) investigated the effect of incorporating ECC with polyvinyl alcohol (PVA) fibers and shape-memory alloys (SMA) on model columns subjected to cyclic loading. Use of PVA-ECC substantially reduced damage in the plastic hinge. Furthermore, the combination of PVA-ECC and SMA led to larger drift capacity compared to the conventional steel reinforced concrete column.

This paper introduces the effectiveness of PFRC for enhancing the damage control and ductility capacity of a full-size bridge column subjected to a strong near-field ground motion using the E-Defense shake table (Kawashima et al. 2012). This column is called herein as C1-6 column. The information obtained from the shake table experiments can provide reliable data for verification of structure performance and can provide an insight on the response of such structures subjected to real earthquake conditions.

2 E-DEFENSE SHAKE-TABLE EXCITATIONS

2.1 *Column configuration and properties*

C1-6 column is a 7.5 m tall, 1.8 m by 1.8 m square, cantilever column shown in Figure 1. It was designed based on the 2002 Japan design code assuming moderate soil condition under the Type II design ground motion (near-field ground motion). PFRC was used at a part of the footing with a depth of 0.60 m below the column base and a depth of 2.7 m above the column base to minimize the cost. The 2.7 m depth of PFRC is three times the code specified plastic hinge length of one-half the column width (0.90 m). This height was set to avoid failure at the PFRC-concrete interface. The 0.60 m depth of PFRC at the footing was provided to minimize damage. Regular concrete with design compressive strength of 30 MPa was used in the other parts of the column. The actual 28-day cylinder compressive strength of concrete was 41 MPa.

The design compressive strength of PFRC was 40 MPa. PFRC was made by combining cement mortar, fine aggregates with maximum grain size of 0.30 mm, water and 3% volume of polypropylene fibers. Monofilament polypropylene fibers with diameter of 42.6 μm, length of 12 mm, tensile strength of 482 MPa, Young's modulus of 5 GPa and density of 0.91 kg/m^3 were used (Hirata et al. 2009). Superplasticizers were added to improve the workability of the mix. The actual 28-day cylinder compressive strength of PFRC was 36 MPa with a strain at peak of 0.47%.

Eighty-35 mm diameter deformed longitudinal bars were provided in two layers. The corresponding reinforcement ratio ρ_l was 2.47%. The nominal yield strength of longitudinal bars was 345 MPa (SD345) and the actual yield strength was 386 MPa at 0.2% strain. Deformed 22 mm diameter ties with 135 degree bent hooks lap-spliced with 40 times the bar diameter

were provided. The outer ties were spaced at 150 mm and the inner ties were spaced at 300 mm throughout the column height. Cross-ties with 180 degree hooks at 150 mm spacing were provided as shown in Figure 1 to increase confinement of the square ties. Volumetric tie reinforcement ratio ρ_s within a height of 2.7 m from the column base was 1.72%. The nominal yield strength of ties was 345 MPa (SD345) and the actual yield strength was 396 MPa at 0.2% strain. Concrete cover of 150 mm was provided.

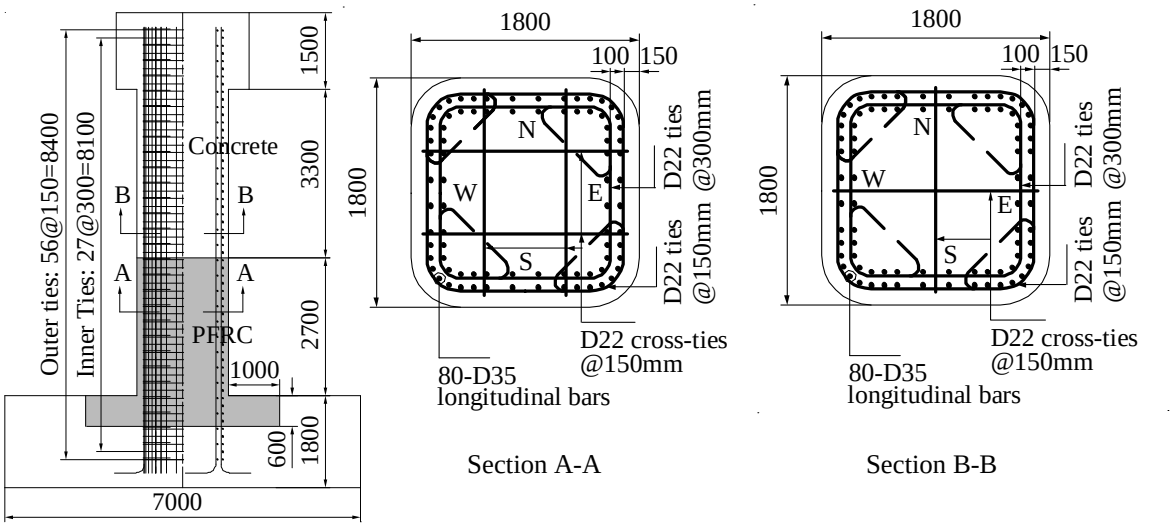

Figure 1. C1-6 column configuration and dimensions (mm)

2.2 *Experiment set-up and shake-table excitations*

Photo 1 shows the experiment set-up using the E-Defense shake table. Four mass blocks were set on the column through two simply supported decks. Note that the decks were not designed to idealize the stiffness and strength of real decks. Each deck was supported by the column on one side and by the steel end support on the other side. Tributary mass to the column by two decks including four weights was 307 tf (3011 kN) and 215 tf (2109 kN) in the longitudinal and transverse directions, respectively. The column was excited using the E-Takatori ground motion with the EW, NS and UD components, shown in Figure 2, applied in the longitudinal, transverse and vertical directions of the column, respectively. This ground motion is referred herein as the 100% E-Takatori ground motion.

Photo 1. Experiment set-up using E-Defense shake table

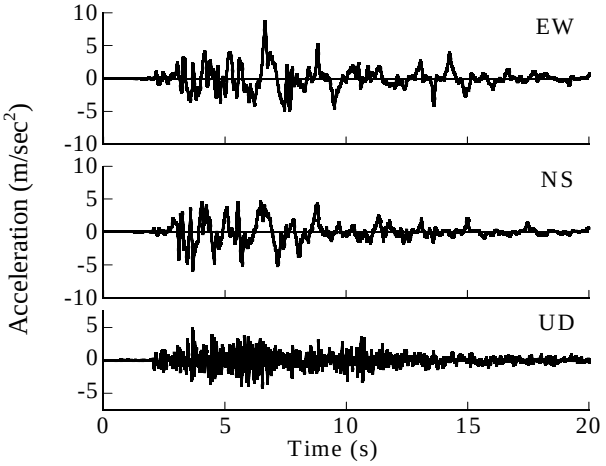

Figure 2. E-Takatori ground motion

Shake table excitations were conducted six times. Excitations were repeated to clarify column performance when subjected to much stronger and longer duration near-field ground motion. The column was excited twice with 100% E-Takatori ground motion (1-100%(1) and 1-100%(2) excitations). After the mass in the longitudinal direction was increased by 21% from 307 tf (3011 kN) to 372 tf (3649 kN), excitations were conducted with 100% E-Takatori ground motion once (2-100% excitation) and 125% E-Takatori ground motion three times (2-125%(1), 2-125%(2) and 2-125%(3) excitations).

3 EFFECT OF POLYPROPYLENE FIBER REINFORCED CEMENT COMPOSITE ON COLUMN SEISMIC PERFORMANCE

3.1 *Progress of failure*

Photos 2 to 4 show the damage progress within 1.2 m from the column base at the SW and NE corner during 1-100%(1), 2-100% and 2-125%(3) excitations at the instance of peak response displacement where the SW corner was subjected to compression while the NE corner was subjected to tension. As shown in Photo 2, during 1-100%(1) excitation, only micro cracks were observed around the column. During 1-100%(2) excitation, very thin flexural cracks as wide as 0.1 - 0.2 mm occurred within 1.6 m from the base all around the column.

During 2-100% excitation, with the mass increased by 21%, damage progressed as shown in Photo 3. Flexural cracks propagated and a crack 0.6 m from the column base at the NE corner opened about 8 mm at the peak response displacement. After the excitation, the maximum residual crack at the above location was 1 - 2 mm wide. Although only flexural cracks occurred all around the column with the cover concrete remaining as a whole shell due to the bridging action of fibers, vertical hairline cracks started to occur at the NE and SW corners within 0.6 m from the column base due to the large strut action of cover concrete shell resulting from the footing reaction when the column was laterally displaced.

During 2-125%(1) excitation, in which the seismic excitation intensity was increased by 25%, at the peak response displacement, the crack 0.6 m from the base opened to 14 mm at the NE corner which was subjected to tension while a vertical crack opened to 9 mm at the opposite SW corner subjected to compression. As the loading progressed, at the SW corner subjected to tension, a crack 1.2 m from the base opened to 9 mm and vertical cracks started to widen at the opposite NE corner.

Succeeding excitations resulted to further propagation of flexural cracks within 2 m from the base around the column and the widening of the vertical crack at the SW corner. As shown in Photo 4, the damage progressed during 2-125%(3) excitation wherein at the peak response displacement, the crack 0.6 m from the base at the NE corner opened to 20 mm and the vertical

crack at the SW corner opened to 15 mm. Note that at the NW corner, cover concrete spalled within 200 mm from the column base when it was subjected to compression while flexural cracks opened to 13 mm at the opposite SE corner subjected to tension. After the excitation, the cracks which opened to over 10 mm during the excitation almost closed with widths of only 5 - 8 mm in flexural cracks and 7 - 12 mm in vertical cracks. Moreover, majority of other small cracks closed to hairline cracks after the excitations due to the fiber bridging action of fibers. Cover concrete spalling was much restricted and there were no exposed longitudinal bars and ties in C1-6 column after 2-125%(3) excitation.

(a) SW corner (b) NE corner

Photo 2. Column damage during 1-100%(1) excitation

(a) SW corner (b) NE corner

Photo 3. Column damage during 2-100% excitation

(a) SW corner (b) NE corner

Photo 4. Column damage during 2-125%(3) excitation

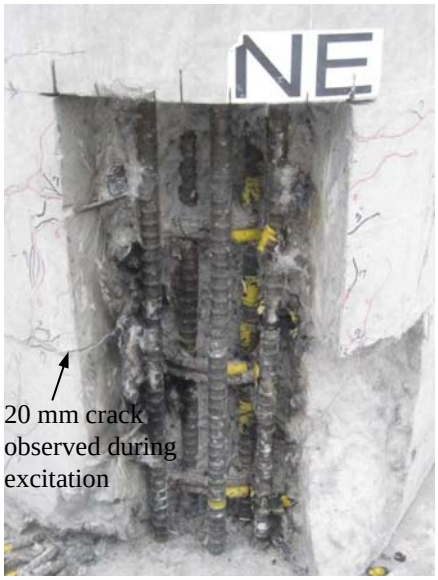

(a) Opened section at NE corner

(b) Longitudinal bar buckling

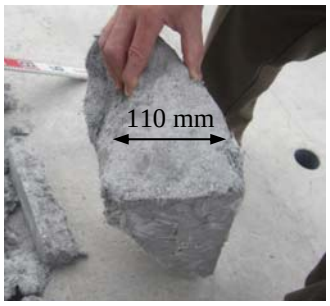

(c) PFRC cover concrete block

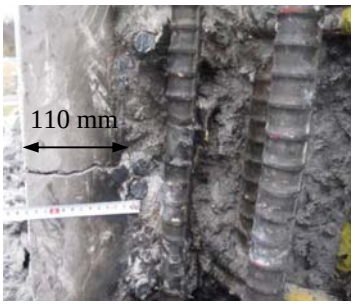

(d) Crack on PFRC cover concrete

Photo 5 Damage of PFRC cover concrete and buckling of longitudinal bars at the NE corner after 2-125%(3) excitation

To investigate how the damage progressed in the core and in the longitudinal bars at the NE corner after 2-125%(3) excitation, the column was opened at the area shown in Photo 5. Note that removal of cover concrete in the fiber mixed concrete was very difficult because of its solid nature compared to that of regular reinforced concrete.

In Photo 5, only the outer and inner longitudinal bars and inner ties can be seen because outer ties and a part of the PFRC cover concrete were removed. Maximum lateral offset among three outer longitudinal bars from their original vertical axis was 8 mm. On the other hand, the inner longitudinal bars did not buckle because they were constrained by the undamaged concrete between the outer and inner longitudinal bars. At the SW corner which was subjected to the largest compression during the peak response displacement, the maximum lateral offset of the outer longitudinal bars due to local buckling was 5 mm which was much less than the buckling of bars at the NE corner. In general, local bar buckling was limited.

At the location where crack opening of 20 mm was observed, it was found that the crack occurred only in the PFRC cover concrete with a depth of 110 mm and did not propagate into the core concrete. Also shown is the block of cover concrete that was removed at the bottom right portion where the presence of fibers held the cover concrete together preventing the disintegration of cover concrete. Hence, it is worthy to note that even after six times of excitation, the damage sustained by C1-6 column was much less than the damage of regular reinforced concrete columns.

3.2 *Response acceleration and displacement*

The principal response angle θ_P is defined to identify the principal response direction when the maximum column response displacement occurs. It is given by

$$\theta_P = \tan^{-1}\left(\frac{u_{TR}}{u_{LG}}\right) \tag{1}$$

where u_{LG} and u_{TR} are the response displacements in the longitudinal and transverse directions, respectively.

Figure 3 shows the acceleration and displacement at the top of column in the principal response direction and Table 1 summarizes the peak acceleration, displacement, residual displacement and moment at each excitation. The principal response angle θ_P varied from 194 to 205 degrees during the six excitations which was almost at the NE-SW direction. The measured peak response acceleration during the series of excitations varied from 13-20 m/s^2.

Due to the high acceleration pulse in the input ground motion, the column experienced high amplitude displacement during each excitation. The peak response displacement was equal to 0.078 m (1% drift) during 1-100%(1) excitation and increased to 0.45 m (6% drift) during 2-125%(3) excitation. As the excitation progressed with increasing intensity of ground motion, the response displacements increased due to column stiffness deterioration resulting from the damage. The residual displacement was only -0.004 m (0.05% drift) after 2-100% excitation, increased to -0.037 m (0.49% drift) after 2-125%(2) excitation then decreased to -0.013 m (0.13% drift) after the last excitation. Since the allowable residual drift for a cantilever column based on the 2002 JRA code is 1%, the residual drift of the column was still smaller than the allowable limit. It is important to note that residual displacement not only increases but also decreases during seismic excitations because it is more affected by the ratio of post elastic stiffness to elastic stiffness as well as the instantaneous structure period (MacRae & Kawashima 1997, Kawashima et al. 19989).

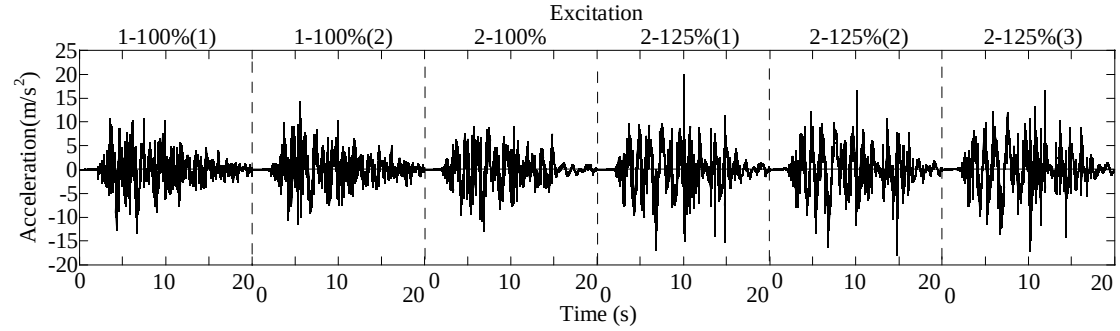

(a) Response acceleration

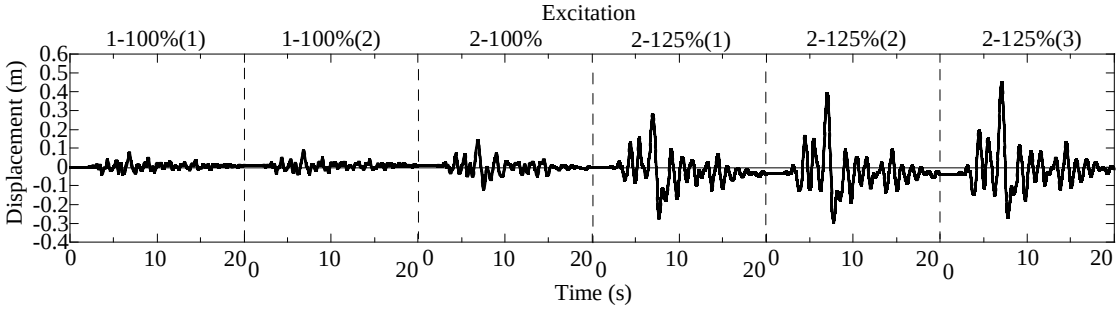

(b) Response displacement

Figure 3. Column response acceleration and displacement in the principal direction

Table 1. Column response in the principal direction

Excitation	θ_P (Degrees)	$\ddot{u}_P$ (m/s^2)	u_P (m)	u_P Drift (%)	Residual displacement (m)	M_P (MNm)
1-100%(1)	201.9	-13.4	0.078	1.0	0.005	20.5
1-100%(2)	193.5	14.2	0.089	1.2	0.007	21.8
2-100%	196.0	-13.0	0.144	1.9	-0.004	24.0
2-125%(1)	201.1	19.9	0.280	3.7	-0.035	24.3
2-125%(2)	204.8	-17.9	0.392	5.2	-0.037	25.3
2-125%(3)	204.6	-17.1	0.450	6.0	-0.013	24.9

3.3 *Moment and ductility capacity*

The bending moment at the column base was evaluated as

$$M_k = M_{Bk} + M_{Ck} \tag{2}$$

where M_{Bk} and M_{Ck} represent the moment based on measured load cell forces and based on pier and column mass accelerations, respectively, and are given by

$$M_{Bk} = \sum_{i=1}^{N} \left\{ F_{Lki} h_{Li} - V_{Li} \left(x_{ki} + u_k \right) \right\} \tag{3}$$

$$M_{Ck} = \int_0^{h_B} m_C \ddot{u}_{Ck} dz + \int_{h_B}^{h} m_B \ddot{u}_{Bk} dz \tag{4}$$

where F_{Lki} is the inertia force measured by the i-th load cell in the k direction (k = LG and TR corresponding to the longitudinal and transverse directions, respectively); V_{Li} is the vertical force measured by the i-th load cell in the k direction; h_{Li} is the height from the base to the i-th load cell; x_{ki} is the load cell coordinate in the k direction from the column center; u_k is the response displacement at top of column in the k direction; N is the load cell number ($N = 32$); z is the coordinate of the column from the base upward; m_C and m_B are the mass per unit length of the column and pier cap, respectively; $\ddot{u}_{Ck}$ is the column acceleration response; $\ddot{u}_{Bk}$ is the pier cap acceleration response; h_B is the height from base to the bottom of the pier cap and h is the height from base to the top of pier cap.

Figure 4 shows the hysteresis of moment at the base vs. displacement at the top of the column in the principal response direction. The hysteresis during the entire six times of excitation is stable with sufficient energy dissipation. As summarized in Table 1, the peak moment gradually increased as the excitation progressed. A maximum capacity of 25.3 MNm at 5.2% drift was developed during 2-125%(2) excitation. During this excitation, flexural cracks further propagated all around the column and the vertical cracks at the SW corner widened as described in 3.1. During the subsequent 2-125%(3) excitation, the peak drift increased to 6% while the peak moment slightly deteriorated by 2%. It should be noted that even during the 2-125%(3) excitation, the moment vs. lateral displacement hysteresis was still very stable.

3.4 *Strains of longitudinal and tie bars*

Figure 5 shows strains of longitudinal and tie bars of C1-6 column at the plastic hinge zone (300-400 mm from the base) at the SW corner where the most extensive damage occurred. Only strains during 1-100%(1), 2-100%, 2-125%(1) and 2-125%(3) excitations are shown due to space limitation. Because longitudinal bars were set in two layers, strains of both the outer and inner longitudinal bars and tie bars are shown here. Noting that the yield strain of both longitudinal and tie bars was nearly 2,000 μ, the longitudinal bars started to yield in tension during 1-100%(1) while tie bars started to yield in tension during 2-125%(1) excitation. The outer and inner longitudinal bars and tie bars exhibited similar response however the amplitude of strains were generally larger in the outer longitudinal and tie bars than the respective inner longitudinal and tie bars.The difference of strain amplitude between outer and inner tie bars is particularly large during and after 2-125%(1) excitation resulting from local buckling of longitudinal bars, which will be described later.

An interesting point in Figure 5 is that the compression strains of the outer and inner longitudinal bars were nearly the same with tension strains during the early excitations. For example, the compression strain of the outer longitudinal bar was 1,800 μ while the tension strain was 1,400 μ during 1-100%(1) excitation. This obviously resulted from the low elastic modulus of PFRC. Resulting from further softening and failure of core concrete, the compression strains of the outer and inner longitudinal bars progressed during 2-125%(1) excitation. Thus, compression strain of the outer longitudinal bar reached 19,000 μ while tension strain reached 18,000 μ during 2-125%(1) excitation. The large compression strain must have caused the outer longitudinal bar to buckle. Note however that in spite of the bar buckling as described in 3.1, spalling of cover concrete did not occur indicating that the presence of fibers made the cover concrete remain as a whole shell.

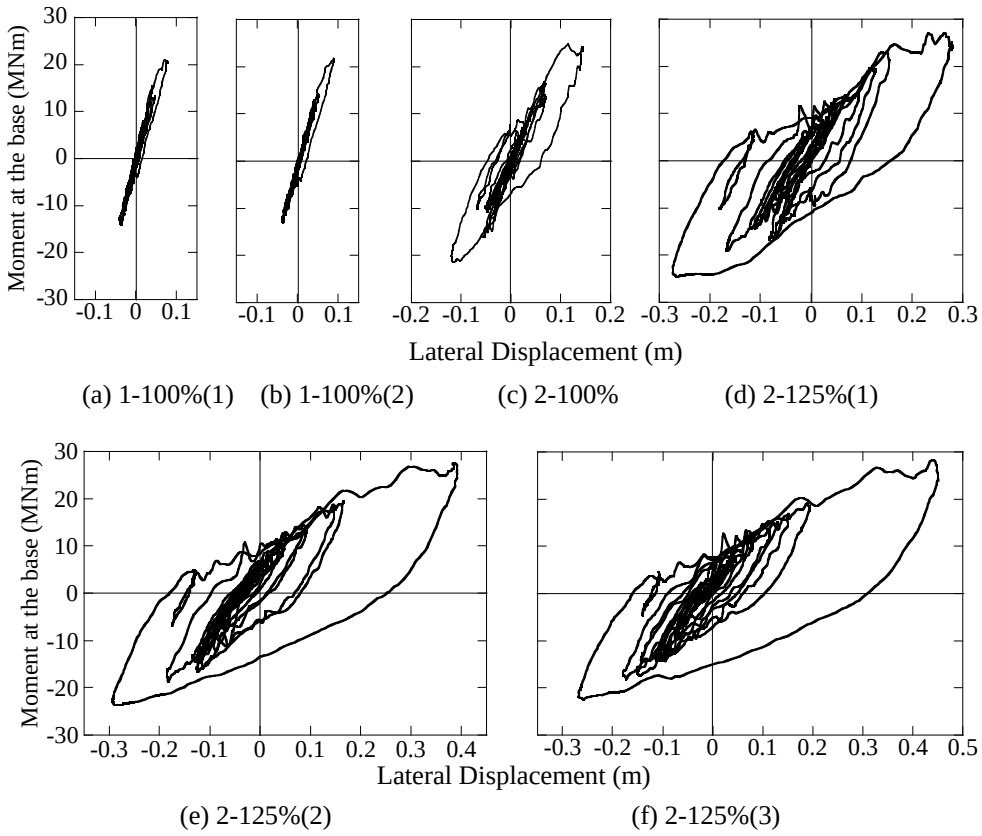

Figure 4. Hysteresis of moment at the base vs. displacement at the top of column in the principal direction

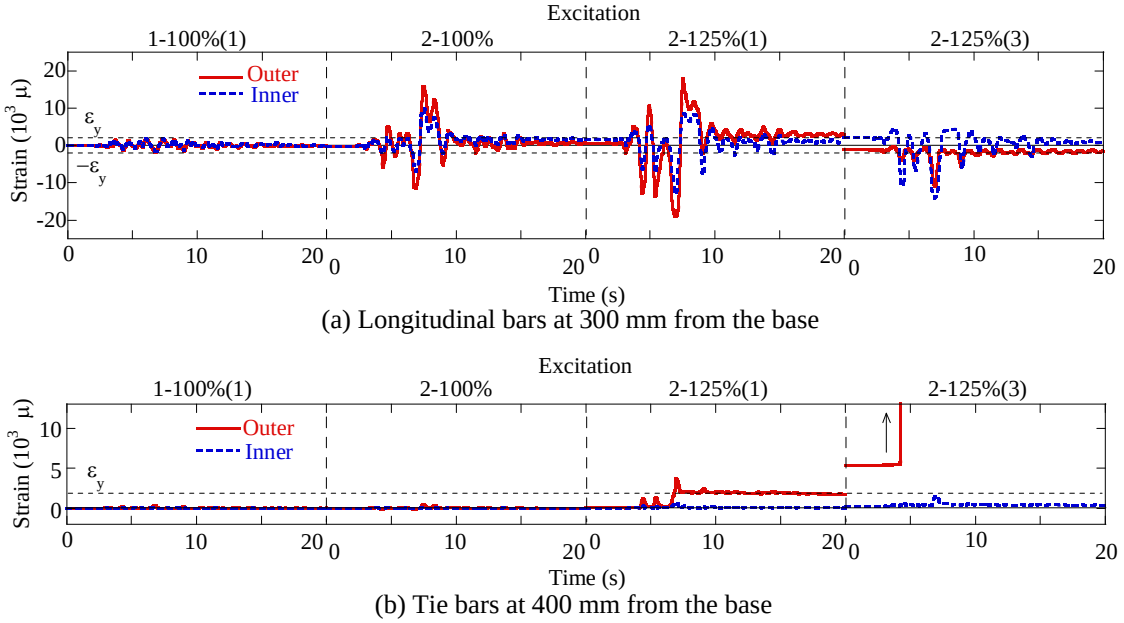

Figure 5. Strains of longitudinal bars and tie bars at the SW corner during 1-100%(1), 2-100%, 2-125%(1) and 2-125%(3) excitations

On the other hand, the tie bar was still elastic during 1-100%(1) until 2-100% excitations. At the instance when compression strain of the outer longitudinal bar sharply increased during 2-125%(1) excitation, the outer tie strain started to increase to 3,700 μ, indicating that the tie resisted the longitudinal bar buckling. Compression strain of the inner longitudinal bar also

sharply increased at the same time, however, the inner tie strain did not increase indicating that the inner longitudinal bar did not buckle. This was because confinement for bar buckling was larger at the inner longitudinal bar than the outer longitudinal bar due to the resistance of core concrete between outer and inner ties which was still intact as shown in Photo 5.

Figure 6 further shows the interaction of a longitudinal bar with a tie bar for outer and inner bars. The tie strains during 2-125%(3) excitation were larger than 5,000 μ and only reliable data are shown here. A sharp increase of the outer tie strain resulting from restraining local buckling of the outer longitudinal bar under high compression strain is clearly seen during and after 2-125%(1) excitation while the inner tie strain remained below 2,000 μ because inner longitudinal bars did not yet buckle.

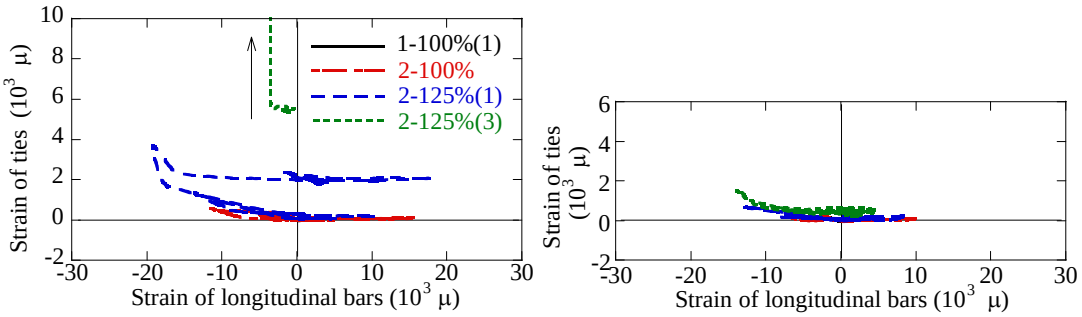

(a) Outer bars (b) Inner bars

Figure 6 Strain of a tie at 400 mm from the base vs. strain of a longitudinal bar at 300 mm from the base at the SW corner of C1-6 column

4 CONCLUSIONS

A series of shake table experiments of a full-size bridge column using polypropylene fiber reinforced cement composites (PFRC) at the potential plastic hinge and part of the footing, referred herein as C1-6 column, were conducted. Based on the results presented, the following conclusions were deduced:

1. PFRC did not have the brittle compression failure of regular reinforced concrete under repeated large inelastic deformation due to the bridging mechanism of fibers. This prevented the brittle crushing of cover and core concrete.
2. As a consequence of a), the use of PFRC reduced buckling of longitudinal bars and deformation of tie bars thus mitigating the damage of C1-6 column even after six times of strong excitations.
3. As a result of the damage mitigation properties of PFRC, the column had a stable flexural capacity and enhanced ductility reaching until 6% drift.

ACKNOWLEDGEMENT

The E-Defense experiments was conducted at the Hyogo Earthquake Engineering Research Center, National Research Institute for Earth Science and Disaster Prevention. A number of research members were involved in the project. The author acknowledges great contribution of Drs. R. Zafra, T. Sasaki, K. Kajiwara, H. Ukon and M. Nakayama for the project.

REFERENCES

Japan Road Association: *Specifications for Highway Bridges*, Maruzen, Tokyo, 2002.

Hirata, T., Kawanishi, T., Okano, M. and Watanabe, S.: Study on material properties and structural performance of high-performance cement composites using polypropylene fiber,*Proc. Japan Concrete Institute* 31(1), 295-300, 2009.

Kawashima, K., MacRae, G. A., Hoshikuma, J. and Nagaya, K.: Residual displacement response spectrum, *Journal of Structural Engineering*, 124(5), 523-530, 1998.

Kawashima, K., Sasaki, T., Ukon, H., Kajiwara, K., Unjoh, S., Sakai, J., Kosa, K., Takahashi, Y., Yabe, M. and Matsuzaki, H.: Evaluation of seismic performance of a circular reinforced concrete bridge column designed in accordance with the current design code based on e-defense excitation, *Journal of Japan Society of Civil Engineers* 65(2), 324-343, 2010.

Kawashima, K., Zafra, R., Sasaki, T., Kajiwara, K. and Nakayama, M.: Effect of polypropylene fiber reinforced cement composite and steel fiber reinforced concrete for enhancing the seismic performance of bridge columns, *Journal of Earthquake Engineering*, 15, 1194-1211, 2011.

Kawashima, K., Zafra, R., Sasaki, T., Kajiwara, K., Nakayama, M., Unjoh, S., Sakai, J., Kosa, K., Takahashi, Y. and Yabe, M.: Seismic performance of a full-size polypropylene fiber-reinforced cement composite bridge column based on E-Defense shake table experiments, *Journal of Earthquake Engineering*, 16, 463-495, 2012.

Kosa, K., Wakita, K., Goda, H. and Ogawa, A.: Seismic strengthening of piers with partial use of high ductility cement. In C. U. Grosse (ed.), *Advances in construction materials*, 269-277, Springer, Berlin Heidelberg, 2007.

Li, V. and Leung, C.: Steady-state and multiple cracking of short random fiber composites, *Journal of Engineering Mechanics*, *ASCE* 118(11), 2246-2264, 1992.

Li, V., Mishra, D. and Wu, H., Matrix design for pseudo-strain-hardening fibre reinforced cementitious composites, *Materials and Structures*, 28, 586-595, 1995.

MacRae, G. and Kawashima, K.: Post-earthquake residual displacements of bilinear oscillators. *Earthquake Engineering and Structural Dynamics*, 26, 701-716, 1997.

Matsumoto, T. and Mihashi, H.: JCI-DFRCC summary report on dfrcc terminologies and application concepts, *JCI International Workshop on Ductile Fiber Reinforced Cementitious Composites – Application and Evaluation*, Takayama, Japan, 2002.

Nakashima, M., Kawashima, K., Ukon, H. and Kajiwara, K.: Shake table experimental project on the seismic performance of bridges using E-Defense, *14th World Conference on Earthquake Engineering*. Paper S17-02-010 (CD-ROM), Beijing, China, 2008.

Saiidi, M., O'Brien, M. and Sadrossadat-Zadeh, M.: Cyclic response of concrete bridge columns using superelastic nitinol and bendable concrete, *ACI Structural Journal*, 106(1), 69-77, 2009.